Electronic supplementary info

Synthesis process and hydrodynamic behavior of a new filtration material for passive wastewater dephosphatation

C. Ruby[*,1,2], K. Barthélémy[1,2], K. Hanna[3,4], M. Mallet[1,2], S. Naille[1,2]

[1] *Université de Lorraine, Laboratoire de Chimie Physique et Microbiologie pour l'Environnement (LCPME), UMR 7564, 405 rue de Vandœuvre, F-54600 Villers-lès-Nancy, France.*

[2] *CNRS, Laboratoire de Chimie Physique et Microbiologie pour l'Environnement (LCPME), UMR 7564, 405 rue de Vandœuvre, F-54600 Villers-lès-Nancy, France.*

[3] *Ecole Nationale Supérieure de Chimie de Rennes, UMR CNRS 6226, 11 Allée de Beaulieu, CS 50837, F-35708 Rennes cedex 7, France*

[4] *Université Européenne de Bretagne, 4, Boulevard Laennec, F-35700 Rennes, France.*

* Corresponding author. Tel.: +33 (0)3 83 68 52 53; fax: +33 (0)3 83 27 54 44

E-mail address: christian.ruby@univ-lorraine.fr

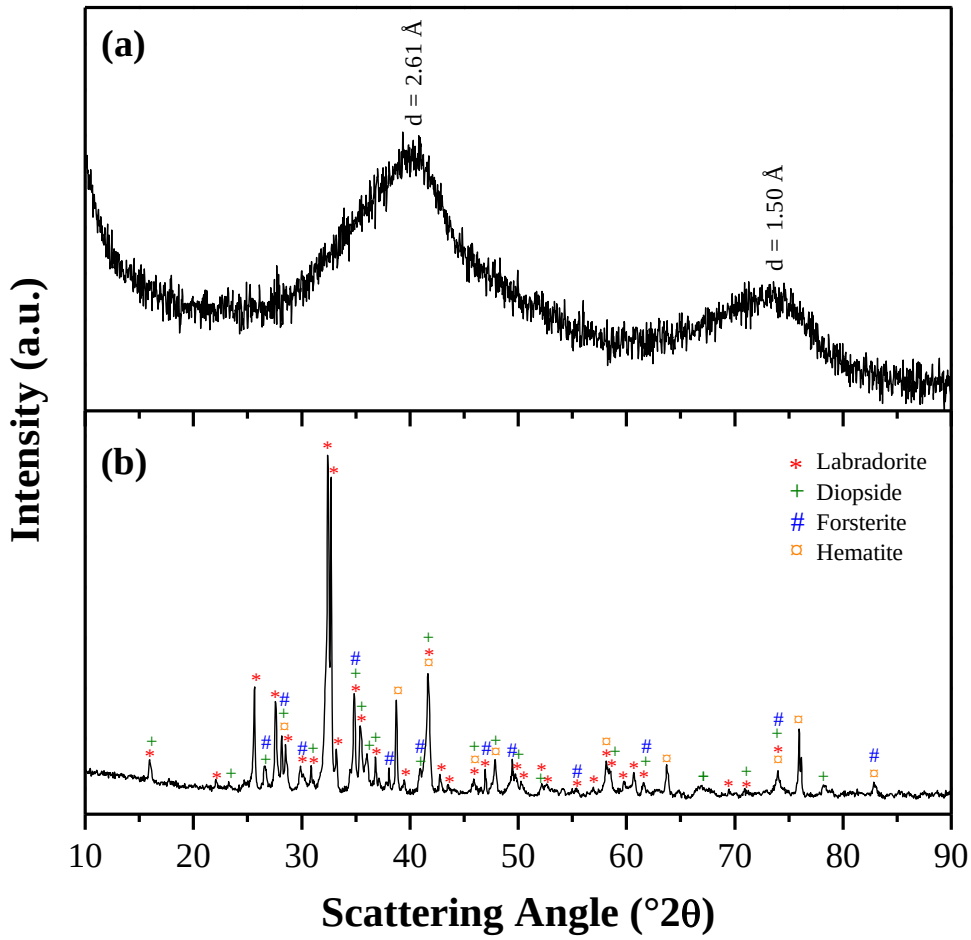

Figure S1. XRD patterns ($\lambda_{\mathrm{CoK}\alpha_1}$ = 1.78897 Å) of (a) pristine ferrihydrite and (b) supplied pozzolana.

Table S1. Characteristics of the five column experiments ([PO_4] = 100 mg L^{-1}; [Cl^-] = 0.1 M).

	Demineralized water			Wastewater	Ca-doped demineralized water
Flow rate (Q, mL min^{-1})	1	0.5	0.1	0.5	0.5
Porous bed length (L, cm)	11.2 ± 0.1	10.5 ± 0.1	10.5 ± 0.1	10.5 ± 0.1	10.5 ± 0.1
Section (S, cm^2)	5.31	5.31	5.31	5.31	5.31
Column volume (V_c, mL)	59.47	55.76	55.76	55.76	55.76
Filter material weight (m, g)	55 ± 0.1	55 ± 0.1	55 ± 0.1	55 ± 0.1	55 ± 0.1
Bulk density (ρ, g cm^{-3})	0.93	0.99	0.99	0.99	0.99
Experimental pore volume (V_p, mL)	40 ± 0.2	40 ± 0.2	40 ± 0.2	40 ± 0.2	40 ± 0.2
Porosity (ϕ, %)	67	72	72	72	72
Darcy velocity (q, cm min^{-1})	0.188	0.094	0.019	0.094	0.094
Pore-water velocity (v , cm min^{-1})	0.281	0.131	0.026	0.131	0.131

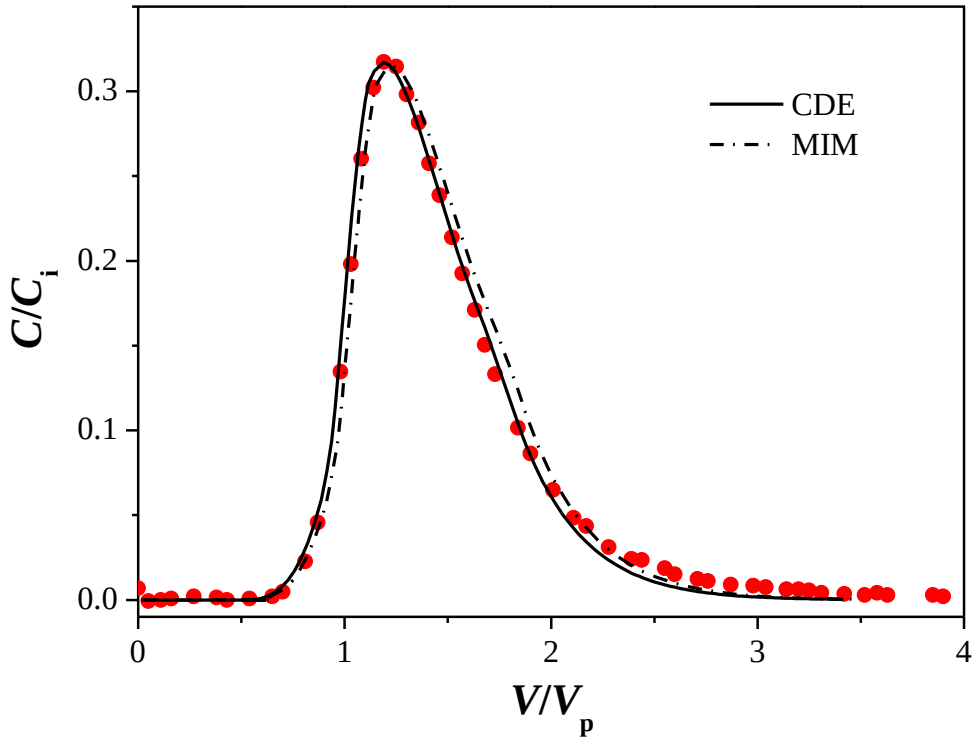

Figure S2. Breakthrough curve of the bromide non reactive tracer for the filter material-packed columns at 0.5 ml min^{-1} flow rate ($[Br^-]$ = 0.01 M). Symbols: experimental data; lines: CDE and MIM fitting.

Figure S2 shows the breakthrough curves of the bromide tracer obtained at 0.5 ml min^{-1}. The pulse injection of bromide produces bell shaped elution curves characterized by a slight asymmetrical shape with little tailing. Diffusion, reflected by the slight flattening, and dispersion phenomena, due to the premature breakthrough, could explain the behavior of the bromide elution.

Modeling of experimental data was performed to determine the hydrodynamic parameters. Analyses can be done using two models, the classical Convection-Dispersion Equation (CDE) and the Mobile-Immobile Model (MIM) [1]. The common assumptions to both models are a constant porosity ϕ over time and no chemical and/or structural material evolution, which implies a constant hydrodynamic dispersion coefficient D.

CDE generally well describes the 1D transport of a nonreactive solute under steady flow conditions in a saturated column. Solute is transported through convection and dispersion by the whole water and then can easily reach all the particles in contact with interstitial water. In this model, the total porosity ϕ_{tot}, which is the volumetric water content

inside the column, is equal to the mobile porosity ϕ_m, which means that all the water is mobile. CDE is expressed as:

$$\frac{\partial C}{\partial t} = D\frac{\partial^2 C}{\partial z^2} - v\frac{\partial C}{\partial z} \quad \text{(S1)}$$

where C is the water solute concentration (mol L^{-1}), t is the time (min), z is the spatial coordinate (cm), D is the hydrodynamic dispersion coefficient (cm^2 min^{-1}) and v the pore-water velocity (cm min^{-1}). The concentration of the nonreactive solute in the outflow was analyzed using CDE developed on MATHCAD Professional software to obtain the values of the hydrodynamic parameters ϕ and D. The macroscopic dispersivity λ (cm) was calculated neglecting molecular diffusion in regards to dynamic dispersion in the studied experimental conditions:

$$\lambda = \frac{D\phi}{q} \quad \text{(S2)}$$

The simulated curve using CDE satisfactorily fits the experimental data (Fig. S2) experimental and theoretical breakthrough points are in relatively good agreement. The hydrodynamic parameters of the saturated columns, deduced by applying Eq. (S1), are reported in Table S2. The macroscopic dispersivity λ is of about 0.34 cm, which is the same order of magnitude than the grain size of Pz (between ~ 0.1 and ~ 0.3 cm). The Peclet number Pe in the columns, defined as:

$$\mathrm{Pe} = \frac{Lv}{D} \quad \text{(S3)}$$

provides information on the relative importance between convection and hydrodynamic dispersion. It was found to be close to 31, indicating a convective regime with non neglecting hydrodynamic dispersion.

The second model, MIM, describes the heterogeneity through water fractionation into a mobile fraction active in mass transport and a stagnant immobile fraction, with convection and dispersion in mobile water and a first-order solute exchange between mobile and immobile fractions due to molecular diffusion. Therefore, the nonreactive solutes concentrations are governed by the following differential equations system:

$$\begin{cases} \phi_m \frac{\partial C_m}{\partial t} + \phi_{im} \frac{\partial C_{im}}{\partial t} = \phi_m D_m \frac{\partial^2 C_m}{\partial z^2} - q\frac{\partial C_m}{\partial z} \\ \phi_{im} \frac{\partial C_{im}}{\partial t} = \alpha\left(C_m - C_{im}\right) \end{cases} \quad \text{(S4)}$$

where ϕ_m and ϕ_{im} are the volumetric water contents of the mobile and the immobile fractions respectively (%), C_m and C_{im} are the relative water solute concentrations in the mobile and the immobile fractions respectively (mol L^{-1}), D_m is the hydrodynamic dispersion coefficient in the mobile fraction (cm^2 min^{-1}), q is the Darcy velocity (cm min^{-1}) and α is the solute exchange rate between the mobile and the immobile fractions (min^{-1}). Bromide concentrations were analyzed using MIM developed on MATHCAD Professional software to provide estimations of the hydrodynamic parameters (ϕ_m, ϕ_{im}, α and D_m). The macroscopic dispersivity λ (cm) was still calculated neglecting molecular diffusion, but this time according to:

$$\lambda = \frac{D_m \phi_m}{q} \tag{S5}$$

Figure S2 shows the theoretical bromide breakthrough curve, modeled from MIM, obtained for 0.5 mL min^{-1} flow rate. Adequate modeling of experimental data is obtained suggesting that MIM could also describe the nonreactive tracer breakthrough curve. A diffusion process might take place in the column. The hydrodynamic parameters for the column are summarized in Table S2. Flow concerns 85 % of total water content (mobile fraction), the other 15 % being immobile.

Table S2. Hydrodynamic parameters modeling with (a) CDE and (b) MIM at 0.5 mL min^{-1} flow rate.

(a)

D (cm^2 min^{-1})	v (cm min^{-1})	λ (cm)	Pe
0.044	0.13	0.34	31

(b)

ϕ_m (%)	ϕ_{im} (%)	α (min^{-1})	λ (cm)
85	15	$2.70\ 10^{-5}$	0.03

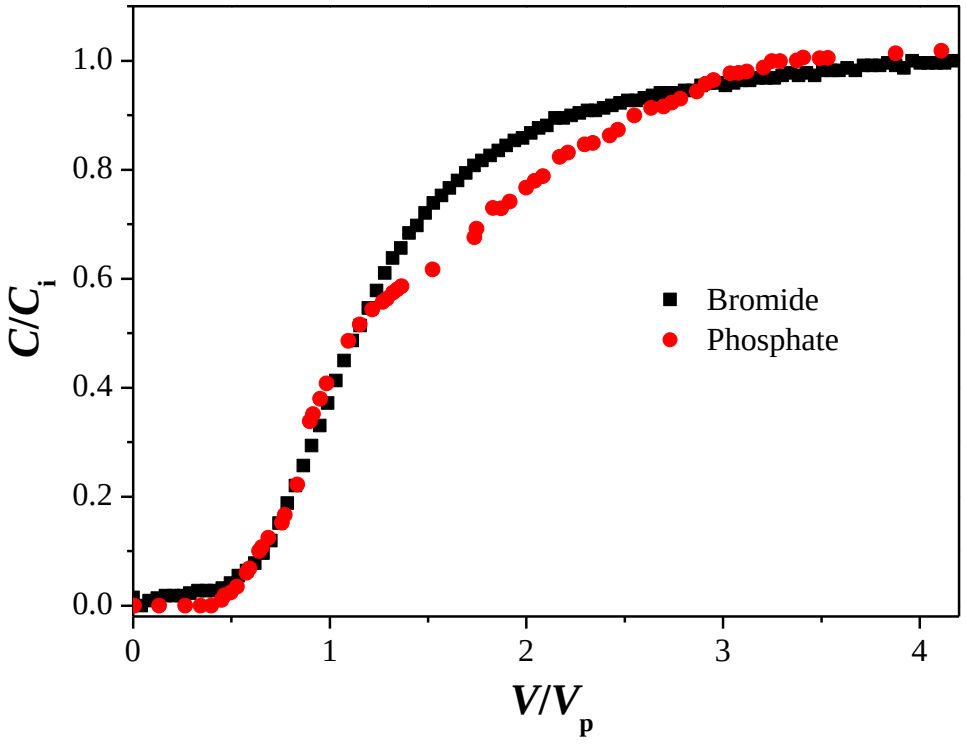

Figure S3. Bromide tracer and phosphate ions breakthrough curves for the filter material-packed columns at 0.5 ml min^{-1} flow rate. For comparison, the phosphate ions breakthrough curve is normalized by its retardation factor to that of the bromide tracer.

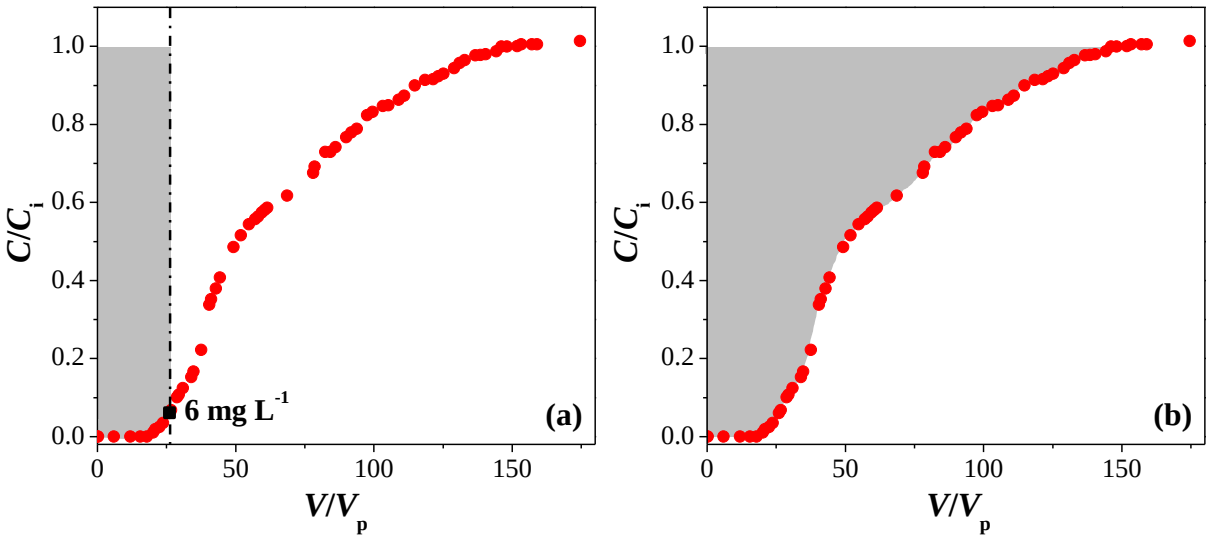

Figure S4. Integration schemes for the calculation of phosphate sorption capacities: (a) calculated from the Council Directive 91/271/EEC and (b) calculated on the entire breakthrough curve.

References

[1] M. Sardin, D. Schweich, F.J. Leij, M.T. van Genuchten, Modeling the nonequilibrium transport of linearly interacting solutes in porous media: A review, Water Resour. Res. 27 (1991) 2287-2307.